Online October 14, 2022
Journal of Neuroendovascular Therapy 2023; 17: 1–7
DOI: 10.5797/jnet.oa.2022-0039

Original Article

Usefulness of 3D T1-Turbo Spin Echo Imaging for the Evaluation of Intracranial Stent Placement

Hiroyuki Mizuno,[1] Masanori Aihara,[1] Koji Sato,[2] Chikashi Negishi,[3] Nobuo Sasaguchi,[2] Hideyuki Kurihara,[2] and Yuhei Yoshimoto[1]

Objective: Evaluation of intracranial stent placement by MRI suffers the problems of signal artifacts during time-of-flight MRA (TOF-MRA). Therefore, angiographic examination is required for detailed intravascular assessment of the stent placement site. Recently, 3D T1-turbo spin echo (3D-TSE) has been developed for evaluation of carotid artery stent placement. We investigated the use of the 3D-TSE imaging method for the evaluation of intracranial vascular stent placement.

Methods: The subjects consisted of nine patients who underwent intracranial vascular stent placement between April 2015 and December 2019. Postoperatively, the lumens of the placed stents were measured by TOF-MRA, DSA, and 3D-TSE imaging. Analysis was performed by type of stent and placement site.

Results: The stents used were Neuroform Atlas (3 patients), LVIS (3 patients), LVIS Jr (2 patients), and Integrity (1 patient). TOF-MRA of the stent placement site showed defects in the image or poor visualization in all nine patients, whereas 3D-TSE imaging visualized the lumen at the stent indwelling site in all patients. The blood vessel diameter measured by the DSA and 3D-TSE imaging exhibited positive correlations regardless of the stent type and placement site.

Conclusion: 3D-TSE imaging allows visualization of the lumen of the site of an intracranial vascular stent, regardless of the type of stent or the vessel. Thus, this method may be useful for evaluating the vascular lumen of a lesion.

Keywords ▶ time-of-flight MRA, 3D T1-turbo spin echo, stent

Introduction

Use of endovascular treatment continues to rapidly increase together with the development of improved devices, and the use of stents in intracranial blood vessels has also increased.[1,2] Angiography is the most reliable and common method for postoperative evaluation of blood vessel status but also requires use of contrast agents, invasion by arterial puncture, and short-term hospitalization. Contrast-enhanced MRA has been reported to yield better results than time-of-flight MRA (TOF-MRA) for the evaluation of the status of the stented artery, but acute adverse events occur in about 1.0% to 2.4% of patients after injection of Gd chelate, and anaphylactic shock and nephrogenic systemic fibrosis have been reported as particularly serious adverse reactions.[3,4] Therefore, non-contrast enhanced intracranial TOF-MRA has been introduced as an alternative evaluation method.[5,6] TOF-MRA is useful for blood flow evaluation before and after stent placement but is strongly affected at the stent placement site by magnetic susceptibility artifacts associated with the gradient echo sequence. Therefore, although TOF-MRA can visualize the lumen of a stented vessel by adjusting parameters, evaluation of such a lumen is generally considered difficult due to signal loss at the stent site.[7]

Non-invasive 3D T1-turbo spin echo (3D-TSE) imaging without contrast medium is a method based on the turbo

[1]*Department of Neurosurgery, Gunma University Graduate School of Medicine, Maebashi, Gunma, Japan*
[2]*Department of Neurosurgery, National Hospital Organization Takasaki General Medical Center, Takasaki, Gunma, Japan*
[3]*Department of Radiation Diagnosis, National Hospital Organization Takasaki General Medical Center, Takasaki, Gunma, Japan*

Received: June 22, 2022; Accepted: September 15, 2022
Corresponding author: Hiroyuki Mizuno. Department of Neurosurgery, Gunma University Graduate School of Medicine, 3-39-22, Showamachi, Maebashi, Gunma 371-8511, Japan
Email: m09201080@gunma-u.ac.jp

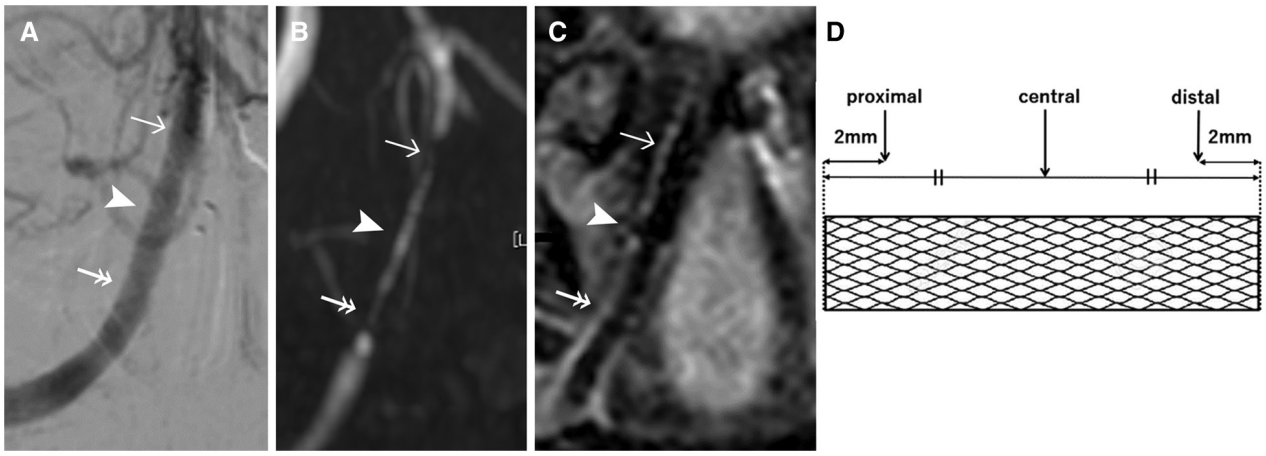

Fig. 1 Case 2. A woman with subarachnoid hemorrhage caused by ruptured right vertebral artery dissecting aneurysm. The left vertebral artery was already occluded by coiling because of ruptured vertebral artery dissection aneurysm. (**A**) Right vertebral angiogram after stent (Integrity) placement showed good patency of the right vertebral artery. (**B**) Postoperative TOF-MRA visualized the stent placement as a signal defect. (**C**) Postoperative 3D-TSE imaging showed the vessel lumen of the vertebral artery at the stent site. Stent proximal (double arrows), stent central (arrowheads), and stent distal (arrows) measurement points. (**D**) Positional relationship between the stent and the measurement point. 3D-TSE: 3D T1-turbo spin echo; TOF-MRA: time-of-flight MRA

spin echo (TSE) sequence, which suffers few magnetic susceptibility artifacts, and is useful for evaluation of the site of carotid artery stent placement, aneurysm occlusions, and atherosclerotic vessels.[8,9] Previous reports have suggested its usefulness for the evaluation of intracranial blood vessels after stent placement, but no detailed reports have included correlation of the vessel diameter with DSA and the effect of the type of stent.[10] Here, we report the use of non-contrast enhanced 3D-TSE imaging for evaluation of intracranial stent placement.

Materials and Methods

The subjects consisted of nine patients who underwent DSA, non-contrast enhanced TOF-MRA, and 3D-TSE imaging at our hospital within one month postoperatively out of 24 patients who underwent intracranial stent implantation between April 2015 and December 2019.

The vascular lumen of the stent was examined by DSA, TOF-MRA, and 3D-TSE imaging methods (**Fig. 1A**–**1C**). The luminal diameter of the blood vessels was measured by each method and the findings compared. Measurements were made at proximal, central, and distal points. The proximal and distal points were located 2 mm inward from the end of the stent, and the central position was located at the center of the stent (**Fig. 1D**).

Cerebral DSA was performed with a biplanar angiographic system (Allura Xper FD20+20; Philips Medical Systems, Eindhoven, the Netherlands). Selective transfemoral injections of the internal carotid or vertebral arteries were performed according to the aneurysm location. All DSA examinations included anteroposterior, lateral, and working views.

MRI was performed using an Ingenia 3.0T (Philips Healthcare, Andover, MA, USA) 16-channel head neck coil. The imaging conditions were as follows: TOF-MRA, field of view 200 mm × 200 mm, matrix 336 × 224, recon voxel size 0.35 mm × 0.35 mm × 0.78 mm, repetition time 24 msec, echo time 3.45 msec, slice thickness 1.2 mm (130 slices), sensitivity-encoding factor 2.8, water-fat shift in pixels/bandwidth in Hz 1.5/288.4, number of excitations 1, and acquisition time 4 min 2 sec, and 3D-TSE imaging, field of view 200 mm × 200 mm, matrix 224 × 224, recon voxel size 0.45 mm × 0.45 mm × 0.45 mm, repetition time 400 msec, echo time 18 msec, TSE factor 20, refocusing control angle 50 degree, slice thickness 0.45 mm (130 slices), sensitivity-encoding factor 4, water-fat shift in pixels/bandwidth in Hz 0.8/539.1, number of excitations 1, spectral presaturation with inversion recovery, and acquisition time 4 min 32 sec. The blood vessel diameter was measured and the blood vessel lumen diameter was compared to establish any correlation.

Measurement of the blood vessel diameter imaged by DSA was performed with a Philips workstation using the auto calibration value of the center of the imager. Measurement of the blood vessel diameter imaged by 3D-TSE imaging was performed using a workstation (VINCENT; Fujifilm Medical, Tokyo, Japan). Histogram analysis of the signal value orthogonal to the blood vessel was performed, and the upper and lower half widths of the signal value were

used to measure the blood vessel diameter. The correlation was reevaluated by categorizing the type of stent used and site of stent placement, and calculating the mean value of the blood vessel diameters measured at the three sites. These measurements were performed by two radiologists unaware of the other parameters of the study.

The image quality of the stented parent artery was graded subjectively on a 3-point scale: 1 = poor (evaluation could not be made), 2 = moderate (evaluation could be made but information was lacking compared with DSA), and 3 = good (image could be evaluated similar to DSA).

Statistical analysis

A Wilcoxon rank-sum test was used to analyze the subjective scores for the quality of the stented artery images. P values <0.05 were considered statistically significant. The weighted κ statistic was used to evaluate the concordance rate of numerical values measured between observers of each method. Correlation between the numbers measured by DSA and 3D-TSE was analyzed using Pearson's product moment correlation coefficient. Statistical analyses were performed with SPSS software, Version 11.5 (SPSS, Chicago, IL, USA).

Ethics approval

This study was approved by the institutional review board of the National Hospital Organization Takasaki General Medical Center and performed in accordance with the ethical standards laid out in the 1964 Declaration of Helsinki and its later amendments. The opt-out information was posted on our homepage prior to inclusion in this study instead of obtaining informed consent from all study subjects. Off-label stents were used with ethics committee approval and family consent preoperatively.

Results

The details of all 9 patients are shown in **Table 1**. The study population consisted of 3 men (33%) and 6 women (67%) with a mean age of 52 years. The diseases consisted of ruptured aneurysm in 7 patients and unruptured aneurysm in 2. The morphology of the aneurysms was saccular in 3 patients (33%), dissection in 4 (44%), and blister in 2 (22%). The types of stent were Neuroform Atlas (Stryker Neurovascular, Fremont, CA, USA) in 3 patients (33%), LVIS (MicroVention-Terumo, Tustin, CA, USA) in 3 (33%), LVIS Jr. (MicroVention-Terumo) in 2 (22%), and Integrity Coronary Stent System (Medtronic, Santa Rosa,

Table 1 Patient characteristics

Case No.	Sex	Location of aneurysm	Rupture	Morphology	Procedure	Stent	Location of stent	Image quality				mRS
								TOF-MRA		3D-TSE		
								Evaluator 1	Evaluator 2	Evaluator 1	Evaluator 2	
1	F	ICA	No	Saccular	SAC	Neuroform Atlas	M2 to C4	Moderate	Moderate	Good	Good	0
2	F	VA	Yes	Dissection	Stenting	Integrity	V4	Poor	Poor	Moderate	Moderate	5
3	F	VA	No	Dissection	Stenting	LVIS Jr	PICA to VA	Moderate	Moderate	Good	Good	0
4	M	VA	Yes	Dissection	Stenting	LVIS	V3 to V4	Poor	Poor	Moderate	Good	3
5	M	ICA	Yes	Blister	Stenting	LVIS	M1 to C2	Poor	Poor	Good	Good	2
6	M	VA	Yes	Dissection	Stenting	LVIS Jr	PICA to VA	Moderate	Moderate	Good	Good	1
7	F	ICA	Yes	Saccular	SAC	Neuroform Atlas	M1 to C3	Good	Good	Good	Good	1
8	F	ICA	Yes	Saccular	SAC	Neuroform Atlas	M1 to C4	Moderate	Good	Good	Good	4
9	F	ICA	Yes	Blister	SAC	LVIS	C1 to C2	Moderate	Moderate	Good	Good	2

3D-TSE: 3D T1-turbo spin echo; C1, C2, C3, and C4: segments of the internal carotid artery defined by Fisher classification; F: female; ICA: internal carotid artery; M: male; M1 and M2: segments of the middle cerebral artery defined by Fischer classification; mRS: modified Rankin Scale; SAC: stent-assisted coiling; TOF-MRA: time-of-flight MRA; V3 and V4: segments of the vertebral artery defined by Fischer classification; VA: vertebral artery

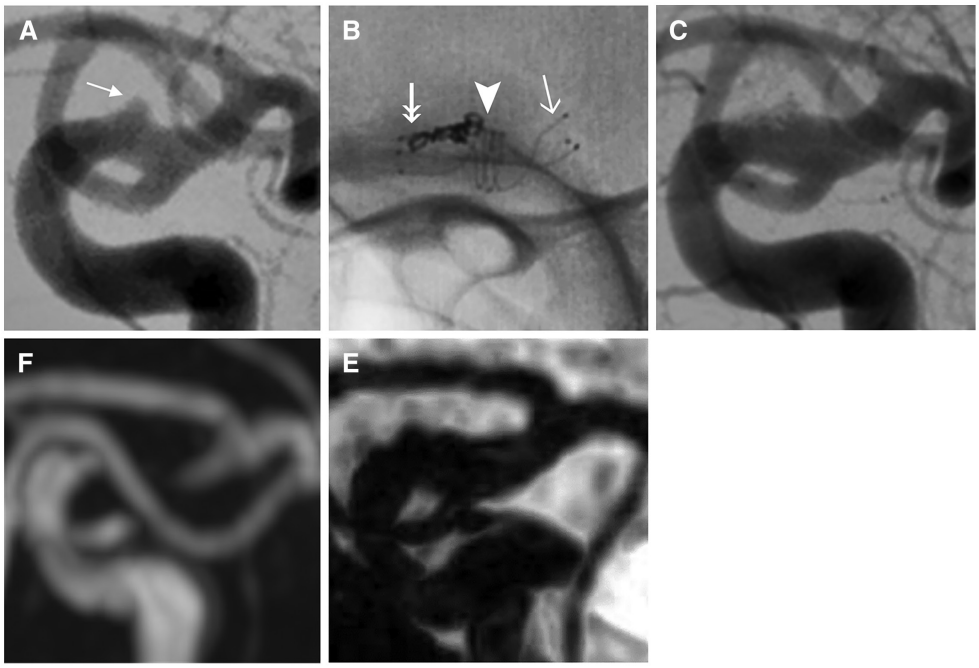

Fig. 2 Case 9. A woman with subarachnoid hemorrhage caused by ruptured blister-like aneurysm arising from the internal carotid artery. (**A**) Preoperative cerebral angiogram showed a blister aneurysm at the anterior wall of the C1 segment of the left internal carotid artery (arrow). (**B**) LVIS stent combined with coiling was deployed successfully. Stent proximal (double arrow), stent central (arrowhead), and stent distal (arrow) measurement points. (**C**) Angiogram just after completion of the procedure showed good patency of the internal carotid artery. (**D**) Postoperative MRA showed metal artifacts of the stent, and the patency of the internal carotid artery was difficult to evaluate. (**E**) 3D-TSE imaging confirmed the patency of the internal carotid artery at the stent site. 3D-TSE: 3D T1-turbo spin echo

CA, USA) in 1 (11%). Stent placement was performed in the intracranial anterior circulation in 5 patients and the posterior circulation in 4. All 9 patients underwent both follow-up MRI and DSA with an interval gap of <14 days. The interval between the follow-up MRI and follow-up DSA was 7.8 ± 1.4 days. The mean period between interventional surgery and follow-up DSA was 120 ± 48 days.

Image quality

TOF-MRA indicated that the stent placement was defective in all nine patients, and the stent location could not be evaluated accurately. In contrast, 3D-TSE imaging confirmed lumen dilation at the stent placement site in all patients. The lumen of the stent could be evaluated regardless of the anterior or posterior circulation of the stent placement site, and even at a site including tortuous blood vessel (**Fig. 2**). Furthermore, the lumen of the blood vessel could be evaluated even if a coil was used in combination with the stent (**Fig. 3**).

Evaluator 1 considered the TOF-MRA image quality to be good in 1 case, moderate in 5, and poor in 3. Evaluator 2 considered the TOF-MRA image quality to be good in 2 cases, moderate in 4, and poor in 3. On the other hand, Evaluator 1 considered the 3D-TSE image quality to be good in 7 cases, moderate in 2, and poor in 0. Evaluator 2 considered the 3D-TSE image quality to be good in 8 cases, moderate in 1, and poor in 0 (**Table 1**). The overall median scores for image quality, in terms of visualization of the stented artery, were 2.0 (interquartile range, 2.5–1.5) and 3.0 (3.0–2.5) for TOF-MRA and 3D-TSE, respectively (P <0.001).

Correlation of the vessel diameter

The blood vessel diameters measured by DSA and 3D-TSE imaging showed high correlations at the proximal, central, and distal sites of the stent (**Fig. 4A**), and for all types of stent used and specific blood vessels (**Fig. 4B** and **4C**). The blood vessel diameter measured by 3D-TSE imaging was approximately 0.8 times that measured by DSA. The modified Rankin Scale score was 0 in 2 patients, 1 in 2, 2 in 2, 3 in 1, 4 in 1, and 5 in 1. Therefore, 6 of the 9 patients had modified Rankin Scale scores of 0–2. The degree of concordance of the measured values between the observers was good with the DSA ($\kappa = 0.87$) and the 3D-TSE ($\kappa = 0.89$) methods. In addition, the values measured by the DSA and 3D-TSE methods showed good correlations with Pearson's correlation coefficient ($r = 0.85$).

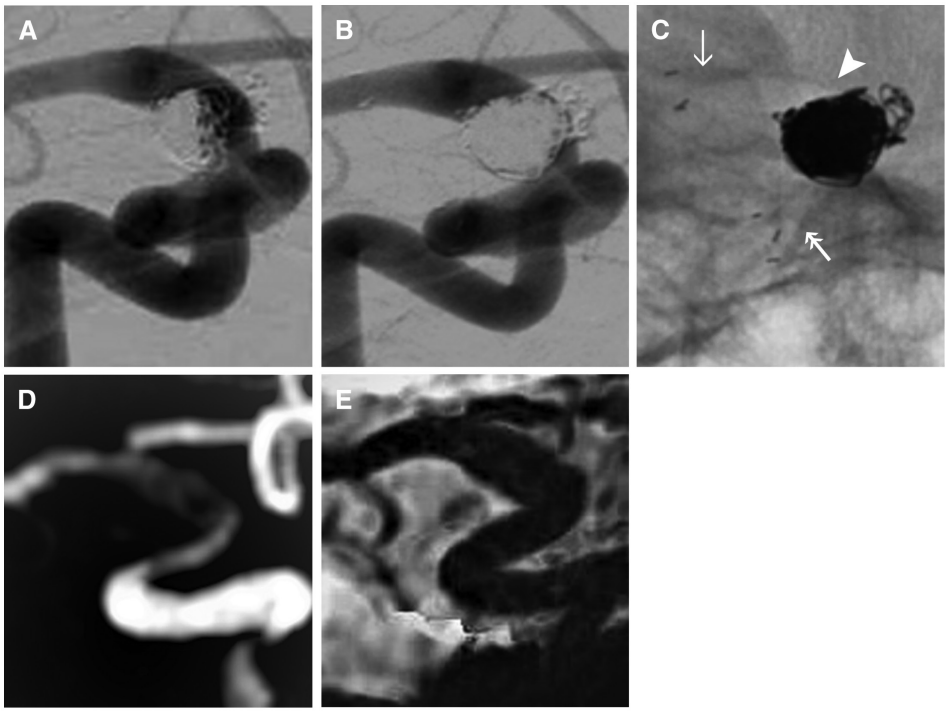

Fig. 3 Case 7. A woman with subarachnoid hemorrhage caused by ruptured recurrent intracranial aneurysm arising from the internal carotid artery-posterior communicating artery bifurcation. (**A**) Initial right carotid angiogram showing a recurrent intracranial aneurysm arising from the internal carotid artery–posterior communicating artery bifurcation. (**B**) Post-procedural angiogram showing almost total obliteration of the aneurysm by stent (Neuroform Atlas)-assisted coil embolization. (**C**) Radiograph after stent-assisted coil embolization for recurrent intracranial aneurysm. Stent proximal (double arrow), stent central (arrowhead), and stent distal (arrow) measurement points. (**D**) Postoperative TOF-MRA visualized the stent placement as a signal defect. (**E**) Postoperative 3D-TSE imaging clearly showed the vascular lumen of the internal carotid artery at the stent site. 3D-TSE: 3D T1-turbo spin echo; TOF-MRA: time-of-flight MRA

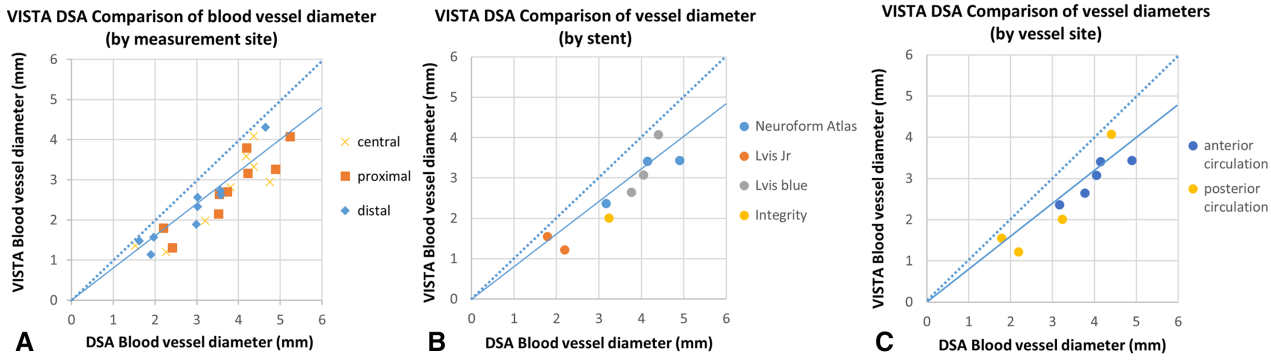

Fig. 4 Comparison of blood vessel diameters measured by the 3D-TSE imaging (VISTA) and DSA methods. Blood vessel diameter classified by the measurement site (**A**), stent (**B**), and blood vessel site (**C**). All values showed high correlations. 3D-TSE: 3D T1-turbo spin echo; VISTA: volume isotropic turbo spin-echo acquisition

Discussion

Since spin echo (SE) methods such as volume isotropic turbo spin-echo acquisition (VISTA) utilize a refocusing pulse, but unlike the gradient echo method such as TOF-MRA, phase disturbance is reduced and the influence of magnetic susceptibility artifacts caused by metal devices can be reduced.[11,12] The name of the 3D-TSE method sequence differs depending on the manufacturer of the MRI: TSE is called VISTA (Philips Medical Systems, Eindhoven, the Netherlands), SPACE (Siemens Healthcare, Erlangen, Germany), or Cube (GE Healthcare, Milwaukee, WI, USA). 3D-TSE, including VISTA, is useful for blood vessel assessment after carotid artery stent

implantation in the case of internal carotid artery stenosis.[9] However, we have found no reports on the utility of the VISTA method for assessment of vessel patency after intracranial artery stent deployment.

The present study found a high positive correlation between the luminal diameters of the blood vessels in the intracranial stent placement site measured by the DSA and 3D-TSE imaging methods. The high correlation with DSA could depend on the matrix size of 0.45 mm and use of isotropic high-resolution imaging, so separation of the blood vessel lumen and blood vessel wall could be easily achieved, and blood vessel diameter was accurately measured.[13] Moreover, the vessel diameter was measured as approximately 0.8 times smaller by the 3D-TSE imaging than the DSA method, possibly due to geometric distortion by the magnetic resonance imager or error due to automatic calibration during DSA measurement. In addition, 2D-DSA uses 2D projection, whereas MRI provides different views derived from thin-slice 2D images.

In addition, the 3D-TSE imaging method allowed evaluation of the vessel diameter regardless of the type of deployed stent, presence or absence of coils, and location of the affected blood vessel. Visualization of the lumen may depend on the material of the stent.[14,15] All four types of stents examined (Neuroform Atlas, LVIS, LVIS Jr., and Integrity) indicated no significant difference with regard to visualization of the lumen, possibly because all four types are made of nickel alloy, which causes a relatively low degree of artifacts.[15] Future study is necessary to examine the utility of the 3D-TSE imaging method in the case of stents with higher metal coverage ratio such as flow diverter stents.

TOF-MRA may involve saturation of blood signals so that blood vessels that run parallel to the imaging profile may be poorly visualized, such as the carotid siphon and horizontal segment of the middle cerebral artery. Moreover, small blood vessels are difficult to visualize at the perforating branch level. However, 3D-TSE imaging utilizes SE using a refocusing pulse, unlike TOF-MRA, so the phase disturbance is reduced and no significant effect is seen with the blood flow in the horizontal direction or from distal to proximal regions, and small blood vessels such as the perforating branches can be detected and visualized with high spatial resolution.[16] Since 3D-TSE imaging can be performed without regard to the blood flow direction, the method is suitable for the evaluation of intracranial blood vessels. The present results suggest that the 3D-TSE imaging method allows minimally invasive examination of the lumen after placement of a stent in an intracranial blood vessel, allowing evaluation similar to cerebral angiography. However, a limitation of this study is the modest number of cases and absence of cases of stenosis and recurrence. Further studies with larger numbers of patients are necessary to validate our results.

Conclusion

The 3D-TSE imaging method has the potential to evaluate the lumen at the deployment site after intracranial stent placement, regardless of the type of stent or the vessel. The 3D-TSE imaging method is useful as a simple and minimally invasive tool for evaluating the lumen after stent implantation.

Acknowledgments

We thank Keisuke Muradate and Yamato Konishi for their excellent technical support.

Disclosure Statement

The authors report no conflict of interest concerning the materials or methods used in this study or the findings specified in this paper.

References

1) Gross BA, Frerichs KU. Stent usage in the treatment of intracranial aneurysms: past, present and future. *J Neurol Neurosurg Psychiatry* 2013; 84: 244–253.
2) King B, Vaziri S, Singla A, et al. Clinical and angiographic outcomes after stent-assisted coiling of cerebral aneurysms with Enterprise and Neuroform stents: a comparative analysis of the literature. *J Neurointerv Surg* 2015; 7: 905–909.
3) Soize S, Gawlitza M, Raoult H, et al. Imaging follow-up of intracranial aneurysms treated by endovascular means: why, when, and how? *Stroke* 2016; 47: 1407–1412.
4) Nelson KL, Gifford LM, Lauber-Huber C, et al. Clinical safety of gadopentetate dimeglumine. *Radiology* 1995; 196: 439–443.
5) Bakker NA, Westerlaan HE, Metzemaekers JD, et al. Feasibility of magnetic resonance angiography (MRA) follow-up as the primary imaging modality after coiling of intracranial aneurysms. *Acta Radiol* 2010; 51: 226–232.
6) Hayashi K, Kitagawa N, Morikawa M, et al. Long-term follow-up of endovascular coil embolization for cerebral

aneurysms using three-dimensional time-of-flight magnetic resonance angiography. *Neurol Res* 2009; 31: 674–680.

7) Kato H, Ootani N, Abiru K, et al. Investigating signal loss due to a carotid artery stent in 3D-TOF-MRA. *Magn Reson Med Sci* 2021; 20: 303–311.
8) Inoue K, Maeda M, Umino M, et al. Cervical carotid plaque evaluation using 3D T1-weighted black-blood magnetic resonance imaging: comparison of turbo field-echo and turbo spin-echo sequences. *Eur J Radiol* 2016; 85: 1035–1039.
9) Idogawa A, Abe Y, Yoshikawa K, et al. Utility of non-contrasted T1-weighted three-dimensional fast-spin echo method in the evaluation of carotid stent placement. *Sendai Med Cent J* 2016; 6: 35–39. (in Japanese)
10) Kim S, Kang M, Kim DW, et al. Usefulness of vessel wall MR imaging for follow-up after stent-assisted coil embolization of intracranial aneurysms. *AJNR Am J Neuroradiol* 2018; 39: 2088–2094.
11) Bakker CJ, Bhagwandien R, Moerland MA, et al. Susceptibility artifacts in 2DFT spin-echo and gradient-echo imaging: the cylinder model revisited. *Magn Reson Imaging* 1993; 11: 539–548.
12) Chiba Y, Murakami H, Sasaki M, et al. Quantification of metal-induced susceptibility artifacts associated with ultra-high-field magnetic resonance imaging of spinal implants. *JOR Spine* 2019; 2: e1064.
13) Komada T, Naganawa S, Ogawa H, et al. Contrast-enhanced MR imaging of metastatic brain tumor at 3 tesla: utility of T1-weighted SPACE compared with 2D spin echo and 3D gradient echo sequence. *Magn Reson Med Sci* 2008; 7: 13–21.
14) Duering TW, Tolomeo DE. An overview of superelastic stent design. In: Russell S, Pelton A, eds. Proceedings of the International Conference on Shape Memory and Superelastic Technologies SMST2000. Carrboro: TIPS Technical Publishing, 2001, 585–604.
15) Teitelbaum GP, Bradley WG Jr., Klein BD. MR imaging artifacts, ferromagnetism, and magnetic torque of intravascular filters, stents, and coils. *Radiology* 1988; 166: 657–664.
16) Busse RF, Brau AC, Vu A, et al. Effects of refocusing flip angle modulation and view ordering in 3D fast spin echo. *Magn Reson Med* 2008; 60: 640–649.